Antimalarial drugs based on artemisinin: DFT calculations on the principal reactions

ARTICLE *in* JOURNAL OF MOLECULAR STRUCTURE THEOCHEM · DECEMBER 2005

Impact Factor: 1.37 · DOI: 10.1016/j.theochem.2005.08.010

ELSEVIER

Journal of Molecular Structure: THEOCHEM 756 (2005) 87–95

THEO CHEM

www.elsevier.com/locate/theochem

Antimalarial drugs based on artemisinin: DFT calculations on the principal reactions

Michael G.B. Drew[a,*], John Metcalfe[a,1], Fyaz M.D. Ismail[b]

[a]*School of Chemistry, The University, Whiteknights, Reading RG6 6AD, UK*
[b]*The Medicinal Chemistry Research Group, The School of Pharmacy and Chemistry, Liverpool John Moores University, Liverpool L3 3AF, UK*

Received 25 June 2005; revised 1 August 2005; accepted 1 August 2005
Available online 7 November 2005

Abstract

Theoretical calculations have been carried out on the interactions of several endoperoxides which are potential antimalarials, including the clinically useful artemisinin, with two possible sources of iron in the parasite, namely the hexa-aquo ferrous ion $[Fe(H_2O)_6]^{2+}$ and haeme.

DFT calculations show that the reactions of all endoperoxides considered, with both sources of iron, initially generate a Fe–O bond followed by cleavage of the O–O bond to oxygen radical species. Subsequently, they can be transformed into carbon-centred radicals of greater stability. However, with $[Fe(H_2O)_6]^{2+}$ as the iron source, the oxygen-centred radical species are more likely to react further akin to Fenton's reagent, whereby iron salts encourage hydrogen peroxide to act as an oxidizing agent, and that solvent plays a major role.

In contrast, when reacting with haeme, the oxygen-centred radicals interconvert to more stable carbon-centred radicals, which can then alkylate haeme. Subsequent cleavage of the Fe–O bond leads to stable and inactive antimalarial products.

These results indicate that the reactivity of the endoperoxides as antimalarials is greater with iron hexahydrates for radical-mediated damage as opposed to haeme, which leads to unreactive species. Since only nanomolar quantities of hydrated metal ions could catalyse the reactions leading to damage to the parasites, this could be an alternative or competitive reaction responsible for the antimalarial activity.

Keywords: Artemisinin; Malaria; Density functional theory; Iron; Haeme; Trioxane rings; Pharmacophore.

1. Introduction

Artemisinin (**1**), a natural product isolated from the Chinese herb *Artemisia annua L.* compositae (Qinghao in Chinese or Gae-tong-sook in Korean), has served as a useful prototype for the development of less neurotoxic, third generation antimalarial drugs [1]. The structure of this compound is rare among secondary plant metabolites in that it contains the unusual 1,2,4-trioxane ring system and is exemplified by artemisinin and its unsaturated relative artemisitene [2]. Molecular recognition of this class of compound by blood schizonticides allowing their preferential importation into malaria-infected erythrocytes (via the parasitophorous duct) merits further study, which may in turn allow the design of more selectively toxic analogues.

A detailed understanding of the mechanism of action has previously relied on the analysis of the reaction products when exposed to metal ions, but denying isolation or characterization of reactive intermediates, which are difficult to quantify using currently available fast reaction techniques. In this respect, the quantum mechanical calculations [3–6] are ideally suited to predict the nature of such species until such time they can be followed spectroscopically The initial event whereby artemisinin destroys parasites probably involves cleavage of the endoperoxide bond in the 1,2,4-trioxane ring by a coordinate iron-containing species. Compounds in which the peroxide is replaced by an ether, or when one peroxy oxygen atoms is bioisosterically replaced by a carbon leads to abolition of antimalarial activity [7]. Importantly, a recent DFT study has shown that this reaction proceeds spontaneously for penta-aquo ferrous and ferric ions as well as porphyrins [8]. This study found

* Corresponding author
E-mail address: m.g.b.drew@reading.ac.uk (M.G.B. Drew).
[1] J.M. on leave from IMI Institute for Research and Development, POB 10140, Haifa Bay 26111, Israel

0166-1280/$ - see front matter © 2005 Elsevier B.V. All rights reserved.
doi:10.1016/j.theochem.2005.08.010

little difference in the chemistry of trioxane compounds, which were effective as antimalarials and those, which had a low activity, suggesting that segments of the compounds apart from the pharmacophore allow selective accumulation in parasitized erythrocytes.

Scission of the peroxy linkage within artemisinin to biologically relevant, non-iron transition metal ions such as Co(II), Cu(II), Ni(II), and Mn(II) in the presence of an excess of cysteine [9] suggests that any biomolecule, especially but not exclusively proteins, containing these metals as a prosthetic group, could be additional targets for these types of compounds. Since trace concentrations of the transition metals are sufficient for bioactivation, it can be assumed that electron transfer reactions dominate such cleavages in biological media ruling out ionised forms of the peroxy group (e.g. ROO–) as nucleophiles as the source of drug action.

Importantly, artemisinin and related trioxanes have been found to demonstrate potent activity against selected carcinomas [10], have spurred the construction of new of trioxane-containing drugs that may find utility in treating pathological conditions that accumulate transition metal-containing species and involve oxidative stress.

2. Methods of calculation

The crystal structure of artemisinin has been obtained several times with no significant variations [11–13] and the common structure was used as the starting model for (1) in our calculations. Structures of other molecules (Fig. 1) were built using the Cerius^2 software package [14] and approximate structures were obtained using molecular mechanics minimisation with the default Universal Force Field. The structures were then geometry optimised using the ADF program [15], which was used for model structures containing transition metals and for solvent calculations using the COSMO system. For all elements, the ZORA approximation was used together with the default TZP basis sets using a small core. In addition, Vosko, Wilk and Nusair's local exchange correlation potential was used [16] together with Becke's non-local exchange [17] and Perdew's correlation corrections [18,19]. Unrestricted calculations were performed for the paramagnetic complexes. The reactions, which occur in the presence of Fe (or other heavy atoms), were carried out under conditions where spin is unlikely to be conserved [20]. Thus, the spin states of the products of these reactions were expected to be those with the lowest energy. As this cannot usually be predicted, it proved necessary to consider three different spin states for all compounds containing Fe.

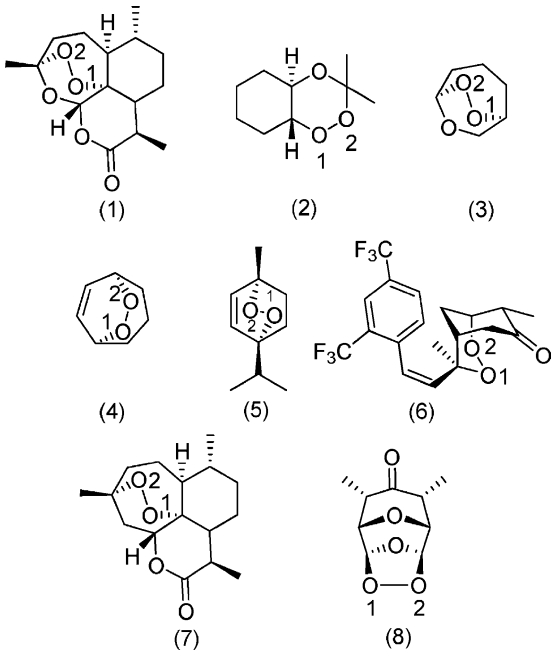

Fig. 1. Endoperoxides considered in this work.

3. Sources of iron and other transition metals in malaria parasites

During its pathogenic intra-erythrocytic phase, *Plasmodium sp.* catabolises host haemoglobin within an acidic food vacuole. Here, globin is digested by a series of protease enzymes [21], and free haeme is released. Consequently, the malaria parasites are highly adapted to cope with the oxidative stress to which they are exposed during the erythrocytic stages of their life cycle. This is achieved by synthesising or sequestering various enzymes including catalase and superoxide dismuase [22]. The parasite initiates a biopolymerisation that produces a microcrystalline centrosymmetric dimer of ferrihaeme to prevent oxidative stress to itself [23]. Intriguingly, in vitro, the haeme cofactor of human iron(II) haemoglobin was efficiently and quickly alkylated by artemisinin at the meso-positions by activation of the peroxide bond forming haeme–artemisinin-derived covalent adducts. [24] These adducts are modelled below (Section 4.2 and Fig. 5).

Egan et al. [25] have speciated the total elemental iron content of unparasitized red cells, parasitized red cells, isolated trophozoites, food vacuoles and haemozoin to determine its distribution amongst these structures. A combination of Mössbauer spectroscopy on freeze-dried trophozoites (to identify the iron species present in the parasite) with electron spectroscopic imaging (ESI) with transmission electron microscopy (TEM) has allowed spatial resolution of elemental iron within cultured *Plasmodium sp*. This study reveals that the parasite food vacuole contains the majority of iron deposited as haemozoin (92 ($\pm$6)%) contradicting the hypothesis that more than 70% of the haematin is oxidatively degraded (by glutathione) [26] or by hydrogen peroxide [27] outside the food vacuole, which could cause iron to enter into the

parasite cytosol (collectively referred to here as the non-haeme 'pool of iron').

Although these speciation experiments suggest that non-porphyrin chelated pool of iron is low (less than 5%), transition-mediated scission of the peroxide bond cannot be discounted since intracellular trafficking of iron with *Plasmodium sp*. will provide the catalytic amounts required for bioactivation reactions, especially if chain branching oxidations are involved. Interestingly, the recent suggestion that haeme iron is not involved in artemsinin bioactivation, based on culturing parasites under an atmosphere of carbon monoxide has not considered the possibility that carbon-centred radicals lead to cell death. Evidence also suggests that haeme iron in the malaria parasite is not needed for the antimalarial effects of artemisinin [28]. This further reinforces the need to perform calculations using various iron species in order to predict interactions of the metal with artemsinin. Importantly, such studies are a necessary prerequisite to spectroscopically identify the transient species involved during interaction of haemin and artemsinin [29].

Investigators [30] continue to employ various iron species as surrogates for haeme to study the types of radicals and breakdown products formed in model systems in order to rationalise antimalarial action. It is likely that such investigations will, at least, improve the warhead portion of the drug and allow production of efficient second and third generation drugs that use artemisinin as the prototype. Pharmacological screening can then be used to study the effects of judicious structural modifications suggested by our modelling investigations.

4. Results and discussion

4.1. Interactions of peroxides with ferrous and ferric compounds

Our previous DFT study [8] has shown that the O–O bond in endoperoxides is cleaved when the endoperoxide interacts with a wide range of metal systems which include the bare Fe(II) and Fe(III) ions and also the complex ions $[Fe(II)(H_2O)_5]^{2+}$, $[Fe(III)(H_2O)_6]^{3+}$, $[Cu(H_2O)_3]^{+}$, and a ferrous porphyrin complex. Notably, the O–O bond was not cleaved when the endoperoxide interacts with $[Zn(H_2O)_5]^{2+}$. Since these results are consistent with the experimental results, it places confidence on the predictive abilities of our calculations for closely related peroxides that are yet to be synthesised. In vitro studies have shown that iron is required for artemisinin to have antimalarial activity [31].

Previous work by ourselves [8], and others [2,3,32,33], on the reactions of artemisinin with iron species has shown that the cleavage of the peroxide bond occurs with the formation of a Fe–O1 bond (which is energetically more favourable than an Fe–O2 bond) and the formation of oxygen radical species. Subsequent reactions will depend on the nature of the iron species. In this present work, we have investigated the reactions of various endoperoxides (see Fig. 1), with two possible sources of iron, namely haeme and the hexa-aquo ferrous ion $[Fe(H_2O)_6]^{2+}$ and these give rise to very different results (vide supra). Potential sources of these species include iron sulphur proteins or oxidative ring scission products of haeme. The iron bound to haemoglobin is primarily in the ferrous state (Fe^{2+}). Catabolic release of haeme results in iron oxidation to the ferric state (Fe^{3+}). Some of the hydrogen peroxide produced during the $Fe^{2+} \rightarrow Fe^{3+}$ conversion may also be used for the peroxidative degradation of haeme. However, a haeme oxygenase capable of releasing free iron is present in *P. berghei* (rodent parasite) and *P. knowlesi* (simian parasite), although it has not thus far been isolated from cultures of *P. falciparum*.

The endoperoxides considered in this work are shown in Fig. 1. In our previous study [8], we considered artemisinin (**1**), *trans*−3,3-dimethyl-1,2,4-trioxadecalin (**2**), and 6,7,8,trioxybicyclo[3,2,2]nonane (**3**). In this investigation, we consider 6,7-dioxabicyclo[3.2.2]non-8-ene (**4**) and the antihelminthic ascaridole (**5**), which have been studied previously [34] as the models for artemisinin, arteflene (**6**) [35], carba-artemisinin (**7**) [36] and the stable ozonide (7,9-dimethyl-3,4,10,11-tetraoxa-tricyclo [4.3.1.12,5]undecan-8-one) (**8**) [37].

4.2. Interactions of endoperoxides with haeme

Previous work [8] has shown that the first step in the interaction of endoperoxides with haeme is likely to be the formation of the Fe–O bond and scission of the O–O bond to give an O-centred radical. With haeme, the O-centred radical converts to a C-centred radical which then alkylates the porphyrin ring in a meso-position [24,35,36] followed by scission of the Fe–O bond though it is not clear whether this proceeds via a concerted process.

In order to investigate the reaction of artemisinin with haeme, we first studied the reaction of (**3**) with a ferrous iron complexed in a porphyrin ring attached to a imidazole molecule (Im) in an axial site, [FeP(Im)], as a model system. It has been shown [8] that the lowest energy of [FeP(Im)(**3**)] was observed when the Fe was bound to O1 (rather than O2) and that this system had preferentially two unpaired electrons. As the alkylated adduct will have no unpaired electrons, the calculations designed to allow this system to carry out the alkylation reaction were made with spin-paired electrons. This reaction is illustrated in Fig. 2. The iron atom has cleaved the O–O bond and the oxygen radical on O2 shown in part (a) reacts to form the more stable carbon radical in (b) which then reacts with a carbon atom in haeme in the meso-position. The resulting structure illustrated in (c) has been geometry-optimised with the ADF program and is stable with a low energy with reasonable dimensions. Importantly, the lowest energy structure is obtained in which the iron has two unpaired electrons.

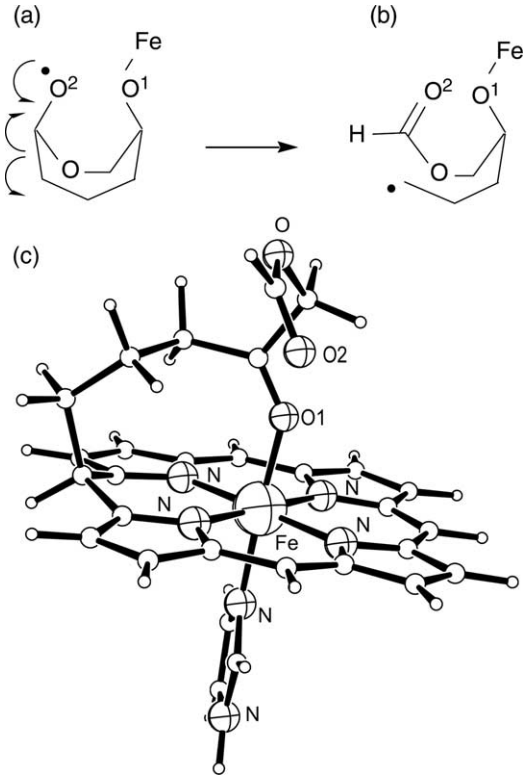

Fig. 2. (a) The iron atom forms the Fe–O1 bond with 3, then breaks the O–O bond to form an oxygen radical on the O2; (b) the oxygen radical rearranges to form a more stable carbon radical and (c) the carbon radical reacts with the haeme in the meso-position and a C–C bond is formed.

ADF calculations on a similar complex with artemisinin (**1**) show that there is no undue strain in the structure and that the structure converged successfully to the arrangement shown in Fig. 3. Again, three different spins were tested and the minimum energy structure contained two unpaired electrons.

An alternative approach is to bind the atom O2 to the metal. The O–O bond will then break, followed by a 1,5 shift (Fig. 4). This will produce a carbon radical, which can then interact with the porphyrin, also in the meso-position, as shown in Fig. 4. However, on this occasion the sequence of atoms in the newly formed ring proceeds from Fe to O2 and then via the artemisinin to the meso-carbon in the porphyrin, and in this case will be shorter by two atoms when bound to O1.

Geometry optimization on artemisinin and the porphyrin separately gave energies of −8.93377, −11.66672 a.u., respectively. The complexes shown in Fig. 3 with O1 bound and Fig. 4 with O2 bound gave energies on the geometry convergence of −20.60469 and −20.60064 a.u., respectively. Thus binding via O1 is favoured by 10.62 kJ mol^{-1} over binding via O2. It is interesting to note that the energy of the complex with O2 bound to the metal is equivalent to the sum of the energies of artemisinin and the porphyrin to within 0.00015 a.u.

The reaction of artemisinin with haeme has been studied experimentally by Meunier et al. [24] (following their work

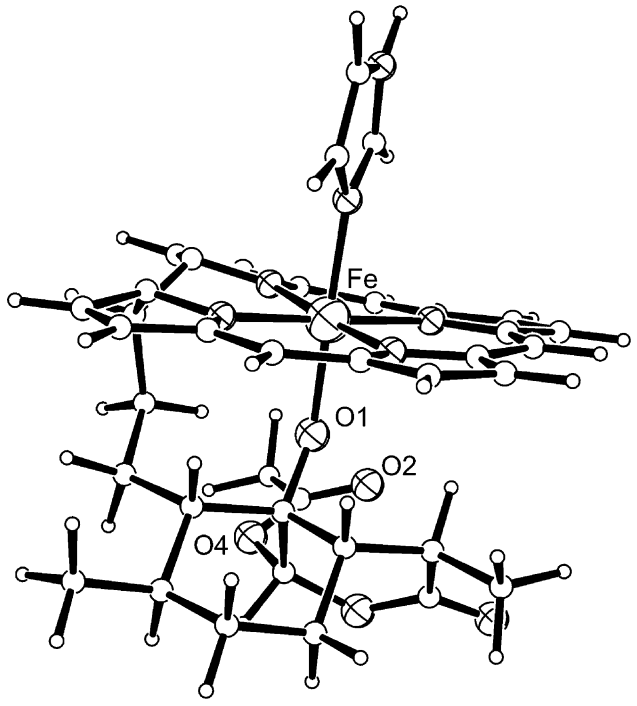

Fig. 3. The structure of [FeP(im)]+ artemisinin bound via O1 showing the C–C bond formed to the porphyrin. Note the induced ruffling in the porphyrin component.

on artemisinin with porphyrins [38,39]) and they have established the presence of four haeme–artemisinin adducts as illustrated in Fig. 5. The four adducts differ in the position of the haeme (a, b, c or d) to which the artemisinin is attached. It is suggested that the mechanism proceeds in

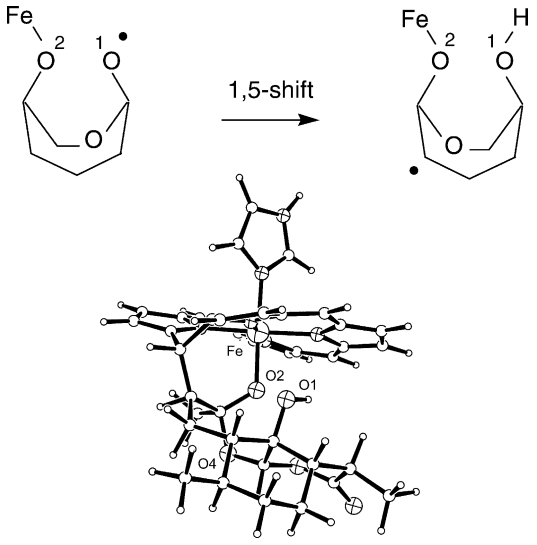

Fig. 4. (a) The iron atom forms a bond to O2.Then the O–O bond is broken to form an oxygen radical on O1; (b) the oxygen radical undergoes the 1,5 H shift to form a more stable carbon radical and (c) the carbon radical reacts with the haeme in the meso-position. Note deviations from planarity induced by binding of artemsinin appended to the porphyrin structure.

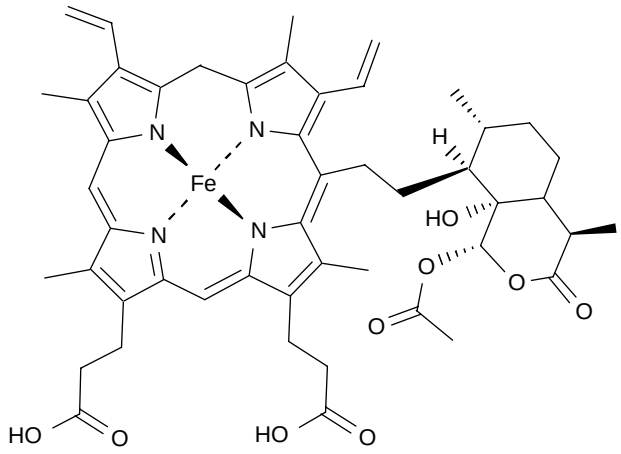

Fig. 5. One of the four possible decomposition products formed following formation of an adduct of artemsinin with haeme as deduced by 2D NMR studies [24].

the manner suggested here, thus via the attachment of O1 to the iron atom of the haeme, the creation of the methylene –CH_2 radical, the joining of the radical to the haeme at position a (or b, c, d), and then the breaking of the Fe–O bond to leave the product illustrated. The overall yield was calculated per haeme residue as 31–33% [24]. Products, which would have been prepared after attachment of O2 to the iron atom, were not observed.

In our calculations with the simpler $[FeP(Im)]^{2+}$ system, the four adducts A, B, C, D are identical as the extra substituents to the porphyrin that characterize haeme are not included.

Most studies of the chemical reactivity of the radicals derived from artemisinin and related compounds have assumed that the activating molecule (usually an iron-containing compound) forms a complex with artemisinin containing the Fe–O bond, which is subsequently broken leaving a reactive derivative of artemisinin in the form of free mono- or bi-radicals. The synthetic work of Meunier et al. [24] and our calculations suggest that the activity of artemisinin is not solely due to its reaction with haeme as this proceeds, after the breaking of the Fe–O bond to a stable covalent product, rather than an active radical of artemisinin which could react further. Also in vitro evidence indicates that the final artemisinin–haeme adduct has little, if any, antimalarial activity [38]. Therefore, it can be suggested that the activity of artemisinin can also be due to its reactivity with a different source of iron (pools of iron) and for that reason interactions with the hydrated iron species are now considered in detail.

4.3. Interactions of endoperoxides with $[Fe(H_2O)_6]^{2+}$

This reaction is similar to the primary reaction in Fenton's reagent, a mixture of hydrogen peroxide and a ferrous (or ferric) ion catalyst. Since a recent DFT study of Fenton's reagent reveals similarity to reactions involving iron and artemisinin, it is included in this discussion [40,41].

4.3.1. Fenton's reagent

The DFT calculations on Fenton's reagent, which is formed by the interaction of ferrous and ferric ions and H_2O_2, have shown that the ferryl ion $[Fe(IV)(H_2O)_5(O^{2-})]^{2+}$ appears to be the main oxidation species [40–44] as proposed by Bray and Gorin [45]. The hydroxyl radical appears to have a very short lifetime in aqueous media as it abstracts a hydrogen atom from either H_2O_2 or from water molecules attached to an iron atom through a hydrogen-bonded chain as soon as it is formed.

The kinetics of oxygen formation in the system iron(III)-hydrogen peroxide has been proposed as an evidence for a hydroxyl radical-mediated chain mechanism [46]. However, that proposed mechanism did not take into account the important effects due to the hydration sphere around the iron(III) that were found in the aforementioned DFT study [40,41]. Our reanalysis of the oxidation results using the reactions from the aforementioned DFT study gives an alternative form for the kinetic equations without the requirement for a hydroxyl radical chain mechanism [46].

4.3.2. Interaction of endoperoxides with $[Fe(II)(H_2O)_6]^{2+}$

In order to simplify the calculations, most were carried out using 6,7,8-trioxobicyclo[3,2,2]nonane (**3**) as a model compound due to its similarity to artemisinin. One important source of ferrous ions species generated within the malaria parasite, apart from those coordinated within haeme, is likely to be $[Fe(II)(H_2O)_6]^{2+}$. Thus, the reaction of the ferrous ion to open the O–O bond will be:

$$[Fe(II)(H_2O)_6]2 + 3 \rightleftharpoons [Fe(II)(H_2O)_4(OH)(3H)]^{2+} + H_2O \quad (1)$$

The species $[Fe(II)(H_2O)_4(OH)(\mathbf{3}H)]^{2+}$ in Eq. (1) arises from the migration of one proton from one of the water molecules bonded to the metal atom to the unattached oxygen atom. The iron cations were given spin states with two unpaired electrons and on convergence, the energy of the species in this reaction are −2.78745 a.u. for $[Fe(II)(H_2O)_6]^{2+}$, −3.89746 for **3** and −6.78069 a.u. for $[Fe(II)(H_2O)_4(OH)(\mathbf{3}H)]^{2+} + H_2O$ combined with a hydrogen bond between the free water molecules and on coordinated to the metal. This gives an energy of −0.10578 a.u. or −277.4 kJ mol^{-1} for this reaction.

This reaction can commence in two ways. Either a water molecule is separated from the hexahydrate and then the pentahydrated iron reacts with **3**, or the iron in the hexahydrate reacts directly with **3** to form initially at least a seven-coordinate species. In the first possible pathway, a water molecule is separated from the iron species and this was investigated by calculating the energy involved in the progressive removal of a water molecule from

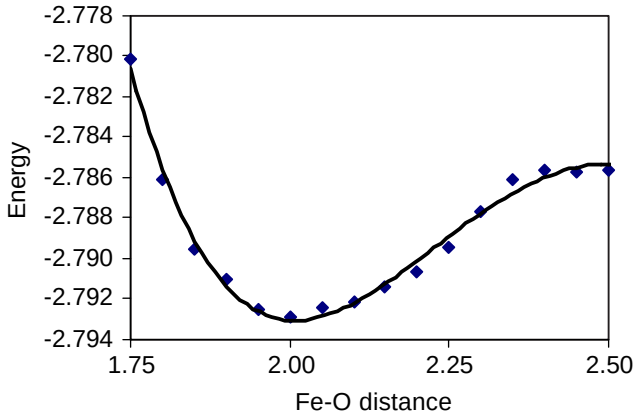

Fig. 6. Fe–O distance (Å) against energy (a.u.) as one bond in $[Fe(OH_2)_6]^{2+}$ is increased in length. Iron has two unpaired electrons.

$[Fe(H_2O)_6]^{2+}$. For this purpose, we used the linear transit option within the ADF program and increased one Fe–O distance within the $[Fe(H_2O)_6]^{2+}$ species in steps of 0.05 Å. The results are shown in Fig. 6.

As can be seen from Fig. 6, the energy barrier for breaking this bond is small (about 16 kJ mol^{-1}) confirming that reaction 1 should proceed readily, facilitating the production of free radicals from the endoperoxides upon exposure to transition metals.

We also considered whether species (**3**) (or an alternative endoperoxide) could attach itself to $[Fe(H_2O)_6]^{2+}$ without necessarily removing a water molecule first. Accordingly the model $[Fe(H_2O)_6(\mathbf{3})]^{2+}$ was built and optimized by molecular mechanics. In order to facilitate the optimization, the bond angle terms around the metal were removed so that van der Waals repulsions were primarily used to generate the minimum energy conformation around the metal atom. O1 was attached to the metal atom. The minimum energy conformation was then geometry optimized (charge 2, spin 2) with the ADF program. After convergence, the structure showed that one water molecule had left the coordination sphere, leaving a six-coordinate Fe complex of formula $[(Fe(H_2O)_4(OH)(\mathbf{3}H)]^{2+}$ as shown in Fig. 8. In this situation, the O–O bond had broken, and a hydrogen atom was migrating from a water molecule on the iron to the terminal oxygen though it is also hydrogen bonded to the oxygen to which it was previously bonded.

If we consider the reaction in Eq. (1), then one can envisage $[Fe(H_2O)_6(\mathbf{3})]^{2+}$ being formed in two ways using Eqs. (1) and (2) shown below with energies in a.u. The asterisks refer to the fact that some dimensions were fixed in these optimizations.

$$\underset{-2.78745}{[Fe(H_2O)_6]^{2+}} + \underset{-3.89741}{3} \rightleftharpoons \underset{-6.69658*}{[Fe(H_2O)_6(3)]^{2+}} \rightleftharpoons \underset{-6.17894*}{[Fe(H_2O)_5(3)]^{2+}} + \underset{-0.51641}{H_2O} \quad (2)$$

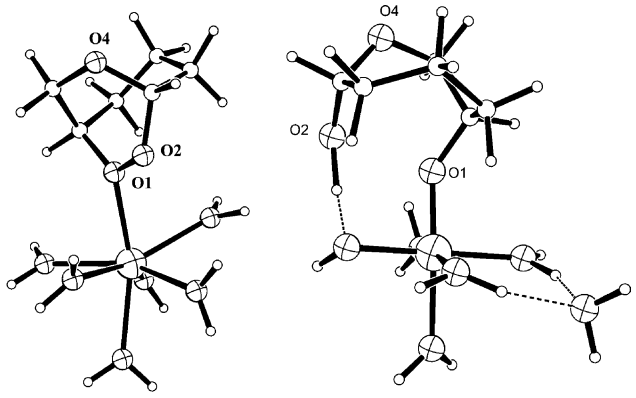

Fig. 7. Starting structure and converged structure for the geometry optimization of $[Fe(H_2O)_6(\mathbf{3})]^{2+}$ with two unpaired electrons. The dotted lines represent O···H interactions.

$$\underset{-2.78745}{[Fe(H_2O)_6]^{2+}} + \underset{-3.89741}{3} \rightleftharpoons \underset{-2.24487}{[Fe(H_2O)_5]^{2+}} + \underset{-0.51641}{H_2O} + \underset{-3.89741}{3} \rightleftharpoons \underset{-6.17894*}{[Fe(H_2O)_5(3)]^{2+}} + \underset{-0.51641}{H_2O} \quad (3)$$

Both Eqs. (1) and (2) are followed by proton transfer taking place from a water molecule in the hydrated iron species $[Fe(H_2O)_5(\mathbf{3})]^{2+}$ to an oxygen radical in **3** so that $[Fe(H_2O)_4(OH)(\mathbf{3}H)]^{2+}$ is formed (Fig. 7).

It proved difficult to obtain the energy of $[Fe(H_2O)_6(\mathbf{3})]^{2+}$ and indeed $[Fe(H_2O)_5(\mathbf{3})]^{2+}$ because on geometry optimization both proceeded to give $[Fe(H_2O)_4(OH)(\mathbf{3}H)]^{2+} + H_2O$, which has an energy of −6.78069 a.u. However, for $[Fe(H_2O)_6(\mathbf{3})]^{2+}$ by fixing the Fe–O(water) bond lengths to be equivalent, it proved possible to obtain a converged energy of −6.69658 a.u. For $[Fe(H_2O)_5(\mathbf{3})]^{2+}$, fixing two O–H bond lengths on the water molecule from which hydrogen transfer can take place allowed geometry convergence to an energy of −6.17894 a.u.

It is interesting to note that this implies that $[Fe(H_2O)_6(\mathbf{3})]^{2+}$ has a lower energy than $[Fe(H_2O)_6]^{2+}$ + **3** by 0.01170 a.u. or 30.77 kJ mol^{-1}. In contrast, $[Fe(H_2O)_6]^{2+}$ is more stable than $[Fe(H_2O)_5]^{2+} + H_2O$ by 0.02617 a.u. or 68.71 kJ mol^{-1}, so it seems likely that the reaction proceeds via Eq. (1) rather than Eq. (2). The relative energies of $[Fe(H_2O)_6(\mathbf{3})]^{2+}$ and $[Fe(H_2O)_5(\mathbf{3})]^{2+} + H_2O$ differ by only 3.24 kJ mol^{-1}.

4.3.3. Comparison of the reactions of the different endoproxides with $[Fe(II)(H_2O)_5]^{2+}$

The calculations involving $[Fe(II)(H_2O)_6]^{2+}$ have shown that it can readily eject one water molecule during the interactions with endoperoxides. It seemed justified, therefore, to simplify the calculations by using $[Fe(II)(H_2O)_5]^{2+}$ directly to study the interactions of the endoperoxides in Fig. 1 with ferrous ions in order to establish whether there were any significant differences.

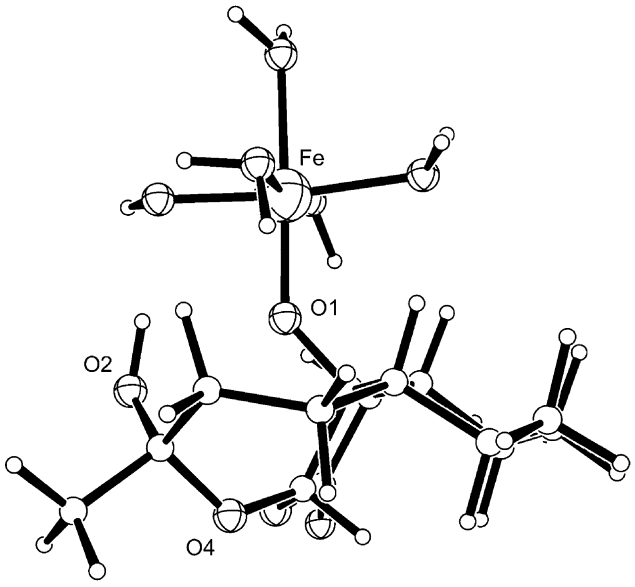

Fig. 8. The structure of the artemisinin complex with $[Fe(H_2O)_5]^{2+}$ after migration of one hydrogen atom from a water molecule to O2.

In the starting models, as with the haeme calculations, the iron atom was bonded to O1 rather than O2 as previous work, [8] suggested that this gave rise to the lowest energy structure. Notably, every bond-breaking event proceeded without energy barriers. Calculations were carried out with different spin states for the iron, and while there was some variation in the nature of the spin state with the lowest energy; in all cases the O–O bond was broken. In each of the examples reported here, migration of one proton had occurred from one of the water molecules bonded to the metal atom to the unattached oxygen atom. An example of such a migration involving artemisinin (**1**) is shown in Fig. 8.

Structural features of the adducts of $[Fe(II)(H_2O)_5]^{2+}$ with the endoperoxides are shown in Table 1. We report details from the calculations with four unpaired electrons. In all structures, the geometry optimization proceeded to convergence with concurrent fission of the O–O bond and creation of a Fe–O bond. As can be seen from Table 1, there is some inverse correlation between the lengths of the Fe–O bond and O···O distance. The O···O distance is clearly

Table 1
Interaction of endoperoxides (**1**)–(**8**) with $[Fe(II)(H_2O)_5]^{2+}$

Compound	Distance (Å)		
	Fe–O(1)	Fe–O(2)	O(1)–O(2)
(1)	1.760	3.568‘	2.442
(**2**)	1.713	4.009	2.610
(**3**)	1.770	3.894	3.458
(4)	1.705	3.237	2.990
(5)	1.699	3.156	2.603
(6)	1.771	3.458	2.621
(**7**)	1.755	3.385	2.365
(**8**)	1.785	3.547	2.868

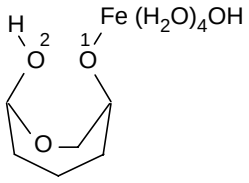

Fig. 9. The complex $[Fe(H_2O)_4(OH)(\mathbf{3}H)]^{2+}$ used in linear transit calculations.

dependent on the steric strain in the endoperoxide. Thus, the longest distance is found for the saturated compound (**3**) followed by (**4**) and (**8**) while the polycyclic molecules such as artemisinin (**1**) and carba-artemisinin (**7**) have the shortest O···O distances.

It would seem from these data that all the endoperoxides described herein interact with Fe(II) in a similar fashion and that there is no significant differences between those compounds known to be biologically active, e.g. (1) and those that are not, e.g. (7). Clearly, the differences in antimalarial activity of the compounds are not due to this first step.

4.3.4. Removal of ferrous ions from activated artemisinin and other endoperoxides

The reactions that could lead to the removal of the activating iron-containing species involve the bond

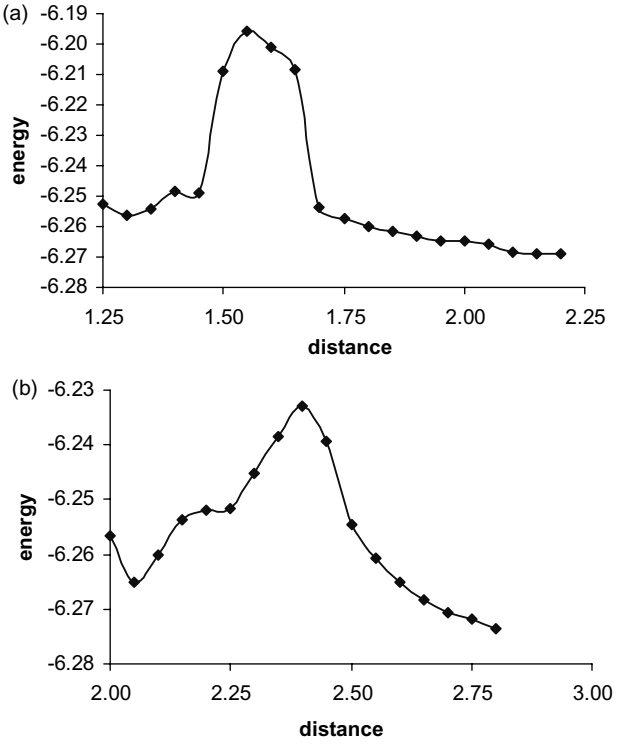

Fig. 10. The respective energy barriers for breaking of (a) the O–C is 159.0 kJ mol^{-1} and (b) the O–Fe bond is 87.0 kJ mol^{-1}. Distances are in Å, energy in a.u.

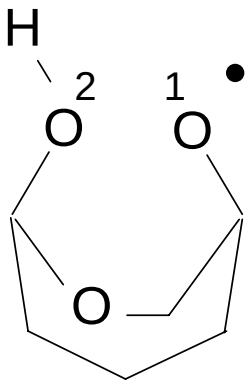

Fig. 11. The oxo-radical **3H**· formed after breaking of the Fe–O bond in the $[Fe(H_2O)_4(OH)(\mathbf{3}H)]^{2+}$ adduct.

breaking of either the Fe–O or O–C bond. As a model, we considered the $[Fe(H_2O)_4(OH)(\mathbf{3}H)]^{2+}$ species shown in Fig. 9. In this molecule either iron species could be removed, either by breaking (a) the Fe–O bond to give $[Fe(H_2O)_4(OH)]^{2+}$ and **3H** or (b) the O–C bond to give $[Fe(H_2O)_4(OH)O]^{2+}$ and a deoxygenated **3H** species. To compare the likelihood of cleaving these two bonds, linear transit calculations were carried out with the ADF program in which the Fe–O and O–C bonds in $[Fe(H_2O)_4(OH)(\mathbf{3}H)]^{2+}$ were elongated at 0.10 Å intervals.

The results are shown in Fig. 10 and show that the energy barrier for breaking the Fe–O bond is very significantly less than that for breaking the O–C bond. This energy barrier will probably be significantly less in an aqueous system due to the action of the solvent stabilising the intermediates but we do not expect this to change the relative energies of these two reactions. Thus, it would seem most likely that the stage of breaking of the Fe–O bond in $[Fe(H_2O)_4(OH)(\mathbf{3}H)]^{2+}$ gives rise to two further species, the Fenton-type reagent $[Fe(H_2O)_4(OH)]^{2+}$ and 3H which is a very reactive active oxo-radical (Fig. 11) which can then react further.

The $[Fe(H_2O)_4(OH)]^{2+}$ species is unlikely to exist as the concerted addition of a water molecule seems likely to give $[Fe(H_2O)_5(OH)]^{2+}$. Ferryl-oxo species have been postulated as being intermediates in the mechanism of action of artemisinin [47] and there is some spectroscopic evidence for their existence [48]. Further reactions of these two reactive species, the oxyradical and the ferryl-oxo species, are being studied and will be reported later.

5. Conclusions

DFT studies provide a vital mechanistic probe in investigating compounds such as artemisinin that lacks strongly absorbing chromophores making spectroscopic investigations difficult. In addition, investigating electron transfer reactions involving species of porphyrins and antimalarial drugs is especially difficult to verify experimentally, but time-resolved resonance studies are planned to investigate such processes [49].

5.1. Implications for peroxide drug design

Two major conclusions can be drawn from the present work that need to be taken into account when designing new endoperoxides for treating malaria, firstly that interactions with haeme lead to loss of potential therapeutic action and secondly that all the endoperoxides seem to undergo the same chemistry in the presence of ferrous ions. Hence, this bioactivation must occur near or in sites sensitive to oxidative stress.

The second result may be interpreted in different ways. It could imply that active concentration of the endoperoxide in the parasite is the main cause of its antimalarial activity as several studies have shown enhanced uptake of the labelled artemisinin and derivatives by parasites. Alternatively it could suggest that competing pathways using hydrated iron species are possible (in addition to haeme) since sensitive parasites do not exclude these trioxanes and hence they do form radicals in the parasite especially where iron could pool which may well include proteins that employ these as cofactors [4,49,50].

5.2. Improved synthesis of 1,2,4 trioxanes

New atom efficient methods to produce 1,2,4 trioxanes hold the promise of reducing the cost of artemisinin type drugs [51]. Calculations could identify the correct minimum pharmacophore that could then be appended to other fragments that will allow modulation of the properties to give the best pharmacodynamic and pharmacokinetic profile in vivo. Additionally, the influence of suitable functional groups could be used to modulate the reactivity of the peroxide bond to find the correct degree of reactivity within the peroxide/trioxane functional group. In this respect, the carbonyl within the stable ozonide (7,9-dimethyl-3,4,10,11-tetraoxa-tricyclo [4.3.1.12,5]undecan-8-one) (**8**) [37] induces remote stabilisation of the ordinarily unstable trioxolane functionality revealing an important design principle that we will be reporting on in the near future.

Acknowledgements

We thank Professors H.M. Frey and I.M. Mills, University of Reading for fruitful discussions and helpful suggestions.

References

[1] J.L. Vennerstrom, S. Arbe-Barnes, R. Brun, S.A. Charman, F.C.K. Chiu, J. Chollet, Y.X. Dong, A. Dorn, D. Hunziker, H. Matile, K. McIntosh, M. Padmanilayam, J.S. Tomas, C. Scheurer, B. Scorneaux, Y.Q. Tang, H. Urwyler, S. Wittlin &, W.N. Charman, Nature 430 (2004) 900.
[2] P. Christen, J.L. Veuthey, Curr. Med. Chem. 8 (2001) 1827.
[3] J.D. Gu, K.X. Chen, H.L. Jiang, J. Leszczynski, J. Phys. Chem. A103 (1999) 9364.
[4] J.D. Gu, K.X. Chen, H.L. Jiang, W.L. Zhu, J.Z. Chen, R.Y. Ji, Chem. Phys. Lett. 277 (1997) 234.
[5] A.G. Taranto, J.W.D. Carneiro, F.G. deOliveira, M.T. de Araujo, C.R. Correa, J. Mol. Struct. (Theochem) 580 (2002) 207.
[6] C. Arantes, M.T. de Araujo, A.G. Taranto, J.W.D. Carneiro, Int. J. Quantum Chem. 103 (2005) 749.
[7] B. Ye, Y.L. Wu, Tetrahedron 45 (1989) 7287.
[8] M.G.B. Drew, J. Metcalfe, F.M.D. Ismail, J. Mol. Struct. (Theochem) 711 (2004) 95.
[9] Y.K. Wu, H.H. Liu, Helv. Chim. Acta. 86 (2003) 3074.
[10] S.R. Meschnick, T.E. Taylor, S. Kamchonwongpaisan, Microbiol. Rev. 60 (1996) 301.
[11] Cerius2 software, Accelerys Inc., San Diego, Calif., USA.
[12] K.L. Chan, K.H. Yuen, H. Takayanagi, S. Janadasa, K.K. Peh, Phytochemistry 46 (1997) 1209.
[13] J.N. Lisgarten, B.S. Potter, C. Bantuzeko, R.A. Palmer, J. Chem. Cryst. 28 (1998) 539.
[14] I. Leban, L. Golic, M. Japelj, Acta. Pharm. Jugosl. 38 (1988) 71.
[15] E.J. Baerends, A. Berces, C. Bo, P.M. Boerrigter, L. Cavallo, L. Deng, R.M. Dickson, D.E. Ellis, L. Fan, T.H. Fisher, C. Fonseca-Guerra, S.J.A. van Gisbergen, J.A. Groeneveld, O.V. Gritsenko, F.E. Harris, D. van Hoek, P.H. Jacobson, G. van Kessel, F. Kootstra, E. van Lenthe, V.E. Osinga, P.H.T. Philipson, D. Post, C.C. Pye, W. Ravenek, P. Ros, P.R.T. Schipper, G. Schreckenback, J.G. Snijders, M. Sola, D. Swerhone, G. te Velde, P. Vernooijs, L. Versluis, O. Visser, E. van Wezenbeek, G. Wiesenekker, S.K. Wolff, T. Woo, T. Ziegler, Velde, ADF2000 program. SCM Inc., Vrije Universiteit, Theoretical Chemistry, Amsterdam, The Netherlands, 2000.
[16] S.H. Vosko, L. Wilk, M. Nusair, Can. J. Phys. 58 (1980) 1200.
[17] A.D. Becke, J. Chem. Phys. 88 (1988) 1053.
[18] J.P. Perdew, Phys. Rev. B33 (1986) 8822.
[19] J.P. Perdew, Phys. Rev. B34 (1986) 7406.
[20] P. Atkins, J. dePaula, Atkins' Physical Chemistry, seventh ed., Oxford University Press, Oxford, 2002.
[21] M. Aikawa, P.K. Hepler, C.G. Huff, H. Sprinz, J. Cell Biol. 28 (1966) 355.
[22] S. Muller, Mol. Microbiol. 53 (2004) 1291.
[23] S. Pagola, P.W. Stephens, D.S. Bohle, A.D. Kosar, S.K. Madsen, Nature (London) 404 (2000) 307.
[24] K. Selmeczi, A. Robert, C. Claparols, B. Meunier, FEBS Lett. 556 (2004) 245.
[25] T.J. Egan, J.M. Combrinck, J. Egan, G.R. Hearne, H.M. Marques, S. Ntenteni, B.T. Sewell, P.J. Smith, D. Taylor, D.A. van Schalkwyk, J.C. Waldon, Biochem. J., Part 2 365 (2002) 343.
[26] H. Ginsburg, O. Famin, J. Zhang, M. Krugliak, Biochem. Pharmacol. 56 (1998) 1305.
[27] P. Loria, S. Miller, M. Foley, L. Tilley, Biochem. J., Part 2 399 (1999) 363.
[28] S. Parapini, N. Basilico, M. Mondani, P. Olliaro, D. Taramelli, D. Monti, FEBS Lett. 575 (2004) 91.
[29] F.M.D. Ismail, M.G.B. Drew, M.J. Dascombe, I. Clark, A.W. Parker. Central Laser Facility, CCLRC Annual Report (2004) 119–120; http://www.clf.rl.ac.uk/Reports/2003-2004/pdf/54.pdf.
[30] G.H. Posner, P.M. O'Neill, Acc. Chem. Res. 37 (2004) 397.
[31] G.H. Posner, C.H. Oh, D.S. Wang, L. Gerena, W.K. Milhous, S.R. Meshnick, W. Asawamahasadka, J. Med. Chem. 37 (1994) 1256.
[32] K.L. Shukla, T.M. Gund, S. Meshnick, J. Mol. Graph Model 13 (1995) 215.
[33] A.G. Taranto, J.W.M. Carneiro, F.G. Oliveira, J. Mol. Struct. (Theochem) 539 (2001) 267.
[34] S.R. Meshnick, T.W. Tsang, F.B. Lin, H.Z. Pan, C.N. Chang, F. Kuypers, D. Chui, B. Lubin, Prog. Clin. Biol. Res. 313 (1989) 95.
[35] J. Cazelles, A. Robert, B. Meunier, J. Org. Chem. 64 (1999) 6776.
[36] M.A. Avery, P.C. Fan, J.M. Karle, J.D. Bonk, R. Miller, D.K. Goins, J. Med. Chem. 39 (1996) 1885.
[37] W.J. Cummins, M.G.B. Drew, J. Mann, E.B. Walsh, J. Chem. Soc. Perkin Trans. 1 (1983) 167.
[38] A. Robert, J. Cazelles, B. Meunier, Angew. Chem. Int. Ed. 40 (2001) 1954.
[39] J.-F. Berrien, O. Provot, J. Mayrargue, M. Coquillay, L. Ciceron, F. Gay, M. Danis, A. Robert, B. Meunier, Org. Biomol. Chem. 1 (2003) 2859.
[40] B. Ensing, F. Buda, P. Blochl, E.J. Baerends, Angew. Chem. Int. Ed. 40 (2001) 2893.
[41] B. Ensing, F. Buda, P.E. Blochl, E.J. Baerends, Phys. Chem. Chem. Phys. 4 (2002) 3619.
[42] F. Buda, B. Ensing, M.C.M. Gribnau, E.J. Baerends, Chem. Eur. J. 7 (2001) 2775.
[43] B. Ensing, E.J. Baerends, J. Phys. Chem. A 106 (2002) 7902.
[44] C. Koutsoupakis, I. Gialou, E. Pavlidou, S. Kapetanaki, C. Varotsis, Arkivoc, Part 13 (2002) 62.
[45] W.C. Bray, M.H. Gorin, J. Am. Chem. Soc. 54 (1932) 2124.
[46] J.F. Perez-Benito, J. Phys. Chem. A 108 (2004) 4853.
[47] H.M. Frey, University of Reading, Private Communication, 2004.
[48] G.H. Posner, S.B. Park, L. Gonzalez, D.S. Wang, J.N. Cumming, D. Klinedinst, T.A. Shapiro, M.D. Bachi, J. Am. Chem. Soc. 118 (1996) 3537.
[49] S. Kapetanaki, C. Varotsis, FEBS Lett. 474 (2000) 238.
[50] H.M. Gu, D.C. Warhurst, W. Peters, Trans. R. Soc. Trop. Med. Hyg. 78 (1984) 265.
[51] S. Kamchonwongpaisan, G. Chandrangam, M.A. Avery, Y. Yuthavong, J. Clin. Invest. 93 (1994) 467.